

Energetics of interplanar binding in graphite

Matthias C. Schabel and José Luís Martins

*Department of Chemical Engineering and Materials Science, University of Minnesota, Minneapolis, Minnesota 55455
and Minnesota Supercomputer Institute, University of Minnesota, Minneapolis, Minnesota 55455*

(Received 20 September 1991; revised manuscript received 18 February 1992)

Results of an *ab initio* density-functional study of interlayer binding in graphite are presented. We obtain good agreement with experimental results for the equilibrium *c*-axis lattice parameter, exfoliation energy, and uniaxial compressibility for this highly anisotropic material. We also present the calculated band structure of graphite.

Graphite is a material with numerous technological applications. It is also of scientific interest as the prototypical two-dimensional solid. Two polymorphic forms are common: hexagonal (or α -) and rhombohedral (or β -) graphite. Hexagonal graphite crystallizes in the Bernal structure (space group D_{6h}^4),¹ with alternating layers of carbon atoms stacking in an *AB* arrangement while β -graphite has *ABC* stacking of the layers.

An interesting characteristic of graphite is the dichotomy in bonding character within and between planes of carbon atoms. Carbon atoms form sp^2 hybridized orbitals in threefold coordination within layers, making a hexagonal net of aromatically stabilized rings. In contrast, the layers themselves are held together by comparatively weak interactions arising from the overlap of partially occupied p_z orbitals perpendicular to the three hybridized orbitals. The bond energies determined from our calculations differ by more than two orders of magnitude, ranging from 50 meV for the interplanar p_z bond to 5.9 eV for an intraplanar sp^2 bond. While the interplanar forces are commonly attributed to a van der Waals type of dynamic interaction between the electrons on adjacent sheets of carbon, a previous study of this using an extended Thomas-Fermi approach showed poor agreement between a fluctuating dipole model and the interlayer bonding in graphite.² Calculations using the local-density approximation³ (LDA) and the linearized augmented-plane-wave (LAPW) method⁴ obtained an interplanar bond energy of 0.2 eV, four times larger than the experimental value.⁵ The LDA cannot describe the dynamical interactions leading to dispersion forces and does not reproduce the long-range $1/r^6$ van der Waals potential for atoms. Thus, if the interplanar binding in graphite was dominated by these interactions, the binding of layers would be poorly described by calculations relying upon the LDA.

The band structure of graphite has been described extensively since it is a prototypical example of a two-dimensional solid. It is well known that an isolated graphitic layer would be a zero-gap semiconductor, while the three-dimensional solid is a semimetal with small electron and hole pockets because of the weak interlayer interaction. There is, nevertheless, a discrepancy between recent self-consistent calculations in the position of the top of the σ band with respect to the Fermi level, E_F . Pseudopotential calculations^{6,7} find that level ~ 3.0 eV

below E_F while LAPW calculations⁴ find it 4.6 eV below E_F .

The present results were obtained using the local-density approximation to density-functional theory,³ within the pseudopotential formalism. All calculations were made using a plane-wave basis. We used the hexagonal allotrope in our calculations because it has a smaller primitive cell with fewer atoms than the rhombohedral form, and the electronic structure and structural properties are not expected to depend significantly on the stacking sequence. Soft, transferable pseudopotentials were generated for C in the ground state, non-spin-polarized ($2s^2 2p^2$) atomic configuration using the method of Troullier and Martins⁸ and a core radius of 1.50 bohrs for both the $2s$ and $2p$ wave functions. The procedure of Kleinman and Bylander for generating separable, nonlocal pseudopotentials was used.⁹ The exchange-correlation functional used was that of Ceperley and Alder¹⁰ as parametrized by Perdew and Zunger.¹¹ The energy cutoff for the plane-wave expansion was $E_{\text{cut}} = 64$ Ry, corresponding to approximately 2000 plane waves at the equilibrium *c*-axis lattice spacing. Large Hamiltonian matrices were diagonalized using an iterative scheme.¹² The self-consistent screening potential was determined in the calculations using both six special \mathbf{k} points¹³ in the irreducible Brillouin zone (IBZ) (generated from a uniform $4 \times 4 \times 2$ mesh in reciprocal space), and forty special points in the IBZ (generated from a $8 \times 8 \times 4$ mesh). Comparison of the two calculations revealed a negligible (~ 3 meV) shift in the band energies with respect to E_F , and a 30-meV shift in cohesive energy. These small values clearly demonstrate convergence of the calculated properties with respect to number of \mathbf{k} points.

In Fig. 1 we present the band structure for α -graphite for the first twenty-four valence bands. The main features agree well with previous band-structure calculations,^{4,6,7,14-16} and with experimental angle-resolved photoemission¹⁷⁻²⁰ and inverse photoemission²⁰⁻²⁵ measurements. There is, however, a notable discrepancy between experimental and theoretical results for the position of the top of the occupied σ band with respect to the Fermi level. We find that the top of this band lies 3.0 eV below E_F , in agreement with previous pseudopotential calculations.^{6,7} In contrast, all-electron LAPW calculations⁴ find it 4.6 eV below the Fermi level, in better agreement with the experimental

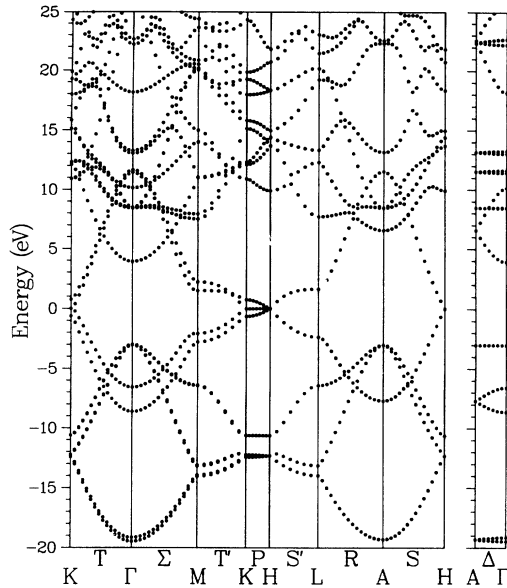


FIG. 1. Electronic band structure of hexagonal graphite calculated for the first 24 bands. The energy zero is at the Fermi level E_F .

value of 4.3 eV below E_F .²⁰ It would be surprising if this ~ 1.6 -eV discrepancy between the pseudopotential and all-electron calculations was due to the pseudopotential approximation. Typically, energy differences in the band structure between numerically converged pseudopotential and LAPW calculations are of the order of a tenth of an eV.²⁶ The authors of the LAPW calculation report that the position of the σ level is very sensitive to the number of \mathbf{k} points used for the Brillouin-zone integration. In contrast, using the scheme of Monkhorst and Pack,¹³ we found rapid convergence of the calculated energy with the number of \mathbf{k} points in the IBZ. For example, the position of the top of the σ band only changes by 3 meV with respect to the Fermi level when the number of \mathbf{k} points in the irreducible wedge of the Brillouin zone is increased from six to forty. Since our calculation is fully converged with respect to size of the basis set and the same should hold for the LAPW calculation, we suspect that the difference in results is due to the different \mathbf{k} -point sampling scheme used in the LAPW calculation.

LDA calculations place the top of the σ band 1.3 eV closer to E_F than is experimentally observed. Since the Fermi level is pinned at the half-filling of the π band, this means that the relative energies of the σ and π bands are incorrectly predicted. This error could be related to the incomplete cancellation of the Hartree self-interaction in the LDA. Because the σ orbitals are more compact than the π orbitals, incomplete cancellation of this interaction will raise the energy of the σ bands with respect to the π bands. An example of this effect is seen in calculations of the electronic structure of ZnS,²⁶ where the localized d electrons of zinc also appear higher in energy relative to the extended s - p band than is experimentally observed.

Minimization of the total energy with respect to the in-plane lattice constant a at constant volume provided

a value of $a_0 = 2.451 \text{ \AA}$, which agrees well with the experimental 0 K value of $a_0 = 2.456 \text{ \AA}$.²⁷ A similar procedure for the axial lattice constant c gives $c_0 = 6.7 \text{ \AA}$ as compared to the empirical value of $c_0 = 6.674 \text{ \AA}$.²⁷ We found that the determination of the dependence of the total energy on c to be significantly more difficult than for the in-plane lattice parameter. This is due to the very small interplanar binding energies ($\sim 25 \text{ meV/atom}$) which lead to sensitivity of the relative energies to numerical noise in the calculation.

We have investigated possible sources of numerical noise in our calculations, and find special precautions necessary in order to obtain consistent results for the interplanar binding energy curve. One source of error is the variation in the dimension of the Hamiltonian matrix with changes in the unit cell geometry. Clearly, when the value of the c/a ratio for the graphite structure is varied the cell geometry also changes. Small discontinuities in the total-energy curves arise at points where the change in cell size results in a corresponding change in the Hamiltonian matrix. This effect is minimized in our calculations by using a large cutoff energy, $E_{\text{cut}} = 64 \text{ Ry}$, and soft pseudopotentials⁸ which exhibit rapid convergence in Fourier space.

The large matrices obtained when the Hamiltonian is expanded in a plane-wave basis are efficiently diagonalized by iterative methods that require only the calculation of the product of the Hamiltonian with a trial wave vector. Explicit calculation of the Hamiltonian matrix can be avoided by observing that the kinetic energy is diagonal, the nonlocal pseudopotential operator may be expressed as a sum of projection operators, and the local potential operator is a convolution which can be calculated with a fast Fourier transform (FFT). If the spatial frequency of the FFT used in the convolution, G_{max} , is twice the maximum spatial frequency included in the plane-wave expansion of the wave functions ($G_{\text{max}} = 16 \text{ a.u.}$ for $E_{\text{cut}} = 64 \text{ Ry}$) the procedure is only limited in accuracy by the computer precision.²⁸ In the intermediate step of the FFT convolution, both the wave function and the potential are calculated on a uniform grid in the unit cell. In the "dual" space formalism¹² the values taken by the wave function on a grid in the crystal unit cell (position representation) and the values of the Fourier components (momentum representation) are considered to be two equivalent representations of the same function. In that case one can argue that the spatial frequency for the FFT convolution may be chosen as small as the spatial frequency of the wave-function sampling ($G_{\text{max}} = 8 \text{ a.u.}$ for $E_{\text{max}} = 64 \text{ Ry}$). This physical approximation introduces a numerical dependency of the calculations on the size of the FFT grid in the crystal unit cell, which is usually small and can be neglected. However, for graphite the small energy scale of the interplanar binding energy means that numerical fluctuations in the total energy of a few meV cannot be tolerated. As the c lattice constant of graphite increases, the density of grid points in the unit cell decreases until there is a jump in the number of grid points of the FFT, which discontinuously increases the density of grid points. At each step in the grid density there is also a correspond-

TABLE I. Morse potential parameters and corresponding physical quantities for our calculations are compared to Thomas-Fermi calculations (Ref. 2), and experimental results. Interplanar binding energy is given by the first parameter E_x and a_0 and c_0 are the lattice constants.

Morse parameters	6 k points	40 k points	6 k points dual space	Thomas-Fermi	Expt.
E_x (meV/atom)	26	24	24	110	22.8 (Ref. 5)
b (\AA^{-1})	0.828	0.783	0.771	0.837	0.971 (Refs. 29 and 30)
c_0 (\AA)	6.55	6.72	6.66	5.58	6.67 (Refs. 29 and 30)
E_c (eV/atom)	8.77	8.80	8.79		7.41 (Ref. 32)
k_c (10^{-12} cm ² /dyn)	3.45	4.11	4.24	1.0	2.7 (Ref. 31)
a_0 (\AA)	2.451				2.456 (Ref. 27)

ing discontinuity in the calculated total energy. We can eliminate this effect by performing calculations with a fixed number of the FFT grid points, but this would lead to effects arising from differences in the grid point density when we calculate binding energy as a function of the c/a ratio. In our calculation of the interplanar binding energy of graphite, we can minimize all these effects by performing calculations with selected values of the c lattice constant which preserve the sampling density of FFT grid points. We have thus performed two types of calculations to obtain the total energy of graphite as a function of the c lattice constant: (i) without the “dual” space and with unconstrained values of the c/a ratio; (ii) with the “dual” space formalism and c/a ratios imposed by the constraint of constant density of FFT grid points.

The total energy of graphite as a function of the c lattice constant is shown in Fig. 2 for values of c/c_0 in the range of 0.80–2.00. The curves calculated using six k points, forty k points, and six k points with the dual space formalism are parallel, with the principal differ-

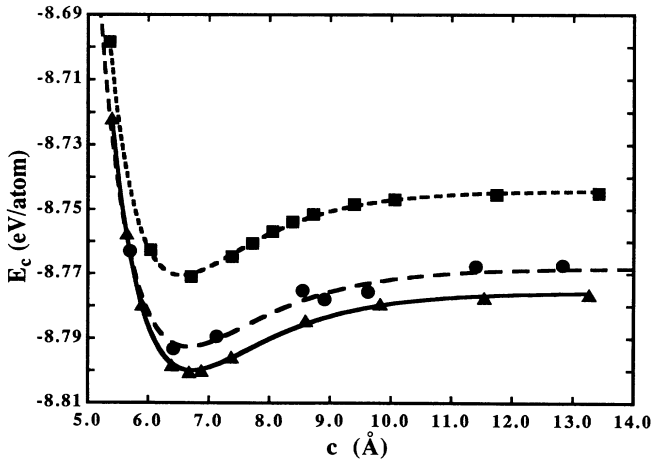


FIG. 2. Calculated total energy plotted vs the c -axis lattice parameter. Three curves are shown corresponding to calculations performed with six special k points in the irreducible wedge of the Brillouin zone to calculate the self-consistent potential (squares), forty k points (triangles), and six k points in combination with the “dual space” method (circles). The energy zero is set at the atomic total energy for carbon, so the minimum represents the cohesive energy E_c for hexagonal graphite. The lines are Morse potential fits to the data points.

ence arising from the 30-meV range (out of 8.8 eV) in the value of the cohesive energy of the isolated graphite plane. The curve with forty k points without the dual space formalism ($G_{\max} = 16$ a.u.) has the highest numerical accuracy. Reducing the number of k points to six shifts the curve upwards by 30 meV. In the curve obtained using the dual space approach with a constant density of FFT grid points in the crystal unit cell one can still see some residual numerical noise at the meV level which is absent from the other two curves. One can also see that the energy of the isolated layer is lowered by 25 meV between the standard and dual space methods for identical k -point sampling. This compensates the shift due to the smaller Brillouin-zone sampling, and it is only by that fortuitous cancelation of errors that the curve appears closer to the most accurate result.

The calculated atomization energy per atom was fitted with a four parameter Morse potential having the functional form $E(c) = E_x \{ \exp[-b(c - c_0)] - 1 \}^2 - E_c$, where E_c is the binding energy of graphite with respect to isolated atoms, and E_x is the binding energy between layers, also called exfoliation energy. The parameters obtained from our data are compared in Table I with both experimental values^{5,29–31} and those from the Thomas-Fermi calculation of DiVincenzo, Mele, and Holzwarth.² It is clear that our data are in very good agreement with experiment, particularly for exfoliation energy, E_x , and c -axis equilibrium lattice constant, c_0 , which are both sensitive to very small energy differences. The uniaxial compressibility is defined by $k_c = (V/c_0^2)(\partial^2 E/\partial c^2)^{-1}$, where V is the volume. In terms of the Morse parameters the uniaxial compressibility is given by $k_c = a_0^2 \sqrt{3}/16 E_x b^2 c_0$. The calculated compressibility of 4.11×10^{-12} cm²/dyn is about 50% in error compared to the experimental value of 2.7×10^{-12} cm²/dyn.³¹

In their extended Thomas-Fermi calculation of interplanar binding, which included a gradient correction to the kinetic energy and used the exchange-correlation functional of Hedin and Lundqvist, DiVincenzo, Mele, and Holzwarth² found difficulty in obtaining quantitative agreement with experimental data. They attributed this to a breakdown of the local-density approximation itself in the regime of low electron density and suggested the necessity of corrections to the correlation energy for accurate prediction of interlayer properties of graphite. LAPW calculations⁴ found a value of 0.14 eV/atom for the interplanar binding energy of graphite. This value

was obtained from the difference in total energy between a slab and a bulk LAPW calculation. The authors mention that adjusting for the systematic differences between the two programs reduces the interplanar binding energy to 0.10 eV/atom, which is still four times larger than the experimental value. In our calculations of the interplanar binding energy of graphite we obtain a very good agreement with the empirical data (Table I), better than should be expected from local-density calculations. The total energy is converged to within 11 meV per atom with respect to basis set size and to within ~ 30 meV per atom with respect to number of special k points. The interplanar binding energy, which is determined by total energy differences, is converged to within ~ 3 meV overall, indicating that our value of 25 meV per atom is numerically sound.

The local-density theory does not include the dynamical effects of dispersive van der Waals interactions. As a consequence, fitting of our total energy data with a four-parameter Lennard-Jones (6-12) potential results in a fit of markedly poorer statistical quality than the Morse potential. Interplanar binding in graphite is often interpreted as arising from a van der Waals type of dipole-induced dipole attraction. However the fact that van der Waals forces are strictly attractive ($1/r^6$ for neutral atoms), implies that, at equilibrium, the repulsive forces must be at least as strong. In graphite the dispersion of the π bands parallel to the c axis, for example, along the A - Γ or the K - H directions, is of the order of 1 eV

(Fig. 1), indicating that the interplanar chemical interactions are not negligible in this system. The fact that our calculations within the framework of local-density theory successfully predict the interplanar binding energy of graphite and reproduce the curvature of the potential well indicates that the contribution of van der Waals forces to the binding of graphite layers is likely a small effect.

In summary, we have calculated the electronic band structure of graphite and have examined the energetics of interplanar binding in this material. We find good agreement between our calculated values for equilibrium c -axis lattice constant, exfoliation energy, and uniaxial compressibility and experimentally determined quantities. We found that special computational precautions become necessary in calculations which require accurate resolution of meV energy differences. With these precautions in mind, we have verified the utility of the local-density approximation for calculating the properties of lamellar materials such as graphite which have pronounced anisotropy in their charge distribution. In addition, our calculations suggest that the binding between planes in graphite is not dominated by van der Waals dispersive interactions.

The authors would like to gratefully acknowledge Professor J. Chelikowsky, Keith Glassford, and Norm Troullier for informative discussions.

-
- ¹J. D. Bernal, Proc. R. Soc. London Ser. A **106**, 749 (1924).
²D. P. DiVincenzo, E. J. Mele, and N. A. W. Holzwarth, Phys. Rev. B **27**, 2458 (1983).
³W. Kohn, and L. J. Sham, Phys. Rev. **140**, A1133 (1965).
⁴H. J. F. Jansen and A. J. Freeman, Phys. Rev. B **35**, 8207 (1987).
⁵L. A. Girifalco and R. A. Ladd, J. Chem. Phys. **25**, 693 (1956).
⁶N. A. W. Holzwarth, S. G. Louie, and S. Rabii, Phys. Rev. B **26**, 5382 (1982).
⁷J.-C. Charlier, X. Gonze, and J.-P. Michenaud, Phys. Rev. B **43**, 4579 (1991).
⁸N. Troullier and J. L. Martins, Phys. Rev. B **43**, 1993 (1991).
⁹L. Kleinman and D. M. Bylander, Phys. Rev. Lett. **48**, 1425 (1982).
¹⁰D. M. Ceperley and B. J. Alder, Phys. Rev. Lett. **45**, 566 (1980).
¹¹J. P. Perdew and A. Zunger, Phys. Rev. B **23**, 5048 (1981).
¹²J. L. Martins and M. L. Cohen, Phys. Rev. B **37**, 6134 (1988).
¹³H. J. Monkhorst and J. D. Pack, Phys. Rev. B **13**, 5188 (1976).
¹⁴A. Zunger, Phys. Rev. B **17**, 626 (1978).
¹⁵R. C. Tatar and S. Rabii, Phys. Rev. B **25**, 4126 (1982).
¹⁶D. A. Fischer, R. M. Wentzcovitch, R. G. Carr, A. Continenza, and A. J. Freeman, Phys. Rev. B **44**, 1427 (1991).
¹⁷P. M. Williams, Nuovo Cimento **38B**, 216 (1977).
¹⁸W. Eberhardt, I. T. McGovern, E. W. Plummer, and J. E. Fisher, Phys. Rev. Lett. **21**, 200 (1980).
¹⁹A. R. Law, J. J. Barry, and H. P. Hughes, Phys. Rev. B **28**, 5332 (1983).
²⁰T. Takahashi, H. Tokailin, and T. Sagawa, Phys. Rev. B **32**, 8317 (1985).
²¹V. Dose, G. Reusing, and H. Scheidt, Phys. Rev. B **26**, 984 (1982).
²²D. Marchand, C. Frétigny, M. Laguës, F. Batallan, Ch. Simon, I. Rosenman, and R. Pinchaux, Phys. Rev. B **30**, 4788 (1984).
²³R. Claessen, H. Carstensen, and M. Skibowski, Phys. Rev. B **38**, 12 582 (1988).
²⁴I. R. Collins, P. T. Andrews, and A. R. Law, Phys. Rev. B **38**, 13 348 (1988).
²⁵F. Maeda, T. Takahashi, H. Ohsawa, S. Suzuki, and H. Suematsu, Phys. Rev. B **37**, 4482 (1988).
²⁶J. L. Martins, N. Troullier, and S.-H. Wei, Phys. Rev. B **43**, 2213 (1991).
²⁷Y. Baskin, and L. Mayer, Phys. Rev. **100**, 544 (1955).
²⁸W. H. Press, B. P. Flannery, S. A. Teukolsky, and W. T. Vetterling, *Numerical Recipes: The Art of Scientific Computing* (Cambridge University Press, Cambridge, 1986).
²⁹H. G. Drickamer, Science **156**, 1183 (1967).
³⁰P. W. Bridgeman, Proc. Am. Soc. Arts Sci. **76**, 9 (1945).
³¹R. Nicklow, W. Wakabayashi, and H. G. Smith, Phys. Rev. B **5**, 4951 (1972).
³²N. N. Greenwood, and A. Earnshaw, *Chemistry of the Elements* (Pergamon, Oxford, 1984), p. 307.